IRREVERSIBLE HIV-1 INACTIVATION EMPLOYING A SMALL-MOLECULE DUAL-ACTION VIROLYTIC ENTRY INHIBITOR STRATEGY

Althea Gaffney[1]*, **Aakansha Nangarlia**[2,3]*, **Steven Gossert**[4]*, Adel A. Rashad[2], Md Alamgir Hossain[2], Cameron F. Abrams[4], Amos B. Smith, III[1], and Irwin Chaiken[2]

[1]Department of Chemistry, University of Pennsylvania, Philadelphia, PA

[2]Department of Biochemistry and Molecular Biology, Drexel University College of Medicine, Philadelphia, PA

[3]School of Biomedical Engineering, Science and Health Systems, Drexel University, Philadelphia, PA

[4]Department of Chemical and Biological Engineering, Drexel University, Philadelphia, PA

*These authors contributed equally.

ABSTRACT

The design, synthesis and validation of a family of small molecule “Dual-Action Virucidal Entry Inhibitors” (DAVEIs) has been achieved that result in irreversible lytic inactivation of HIV-1 virions. These constructs contained two functional components that endow the capacity to bind simultaneously to both the gp120 and gp41 subunits of the HIV-1 Envelope glycoprotein (Env). One component is derived from BNM-III-170, a small molecule CD4 mimic warhead that binds to gp120. The second component, a Trp3 peptide, is a 9-amino acid segment based on the gp41 Membrane Proximal External Region (MPER) that has been proposed to bind to the gp41 MPER domain of the Env. The resulting smDAVEIs both inhibit infection with low micromolar potency and induce lysis of the HIV-1 virion. The lytic activity was selective for functional HIV-1 virions. Crucially, virolysis was found to be dependent on covalent tethering of the BNM-III-170 and Trp3 domains with various spacers, as coadministration of the un-crosslinked components proved not to be lytic. Computational modeling supports a mechanism in which DAVEIs bind to open-state Env trimers and induce relative motion of gp120 subunits that further opens the trimers. Overall, this work represents a promising new step toward the use of small-molecule DAVEIs for eradication of HIV.

INTRODUCTION

Currently over 36.9 million people globally are infected with HIV.[1] While the development of antiretroviral therapies (ARTs) has dramatically increased the life expectancy of these patients, the efficacy of ART is challenged by the cost, the requirement of regular access to care, and the onset of viral resistance. Methods to cure, prevent and eradicate HIV infection are thus urgently needed.[1–5]

The HIV-1 envelope glycoprotein spike (Env) comprises the only HIV-specific protein on the surface of the virion, and consequently is a natural therapeutic target. Env, which regulates viral entry into host cells, is a metastable trimer of non-covalently linked gp120 and gp41 protein subunits.[6] The entry mechanism begins *via* binding of gp120 to CD4, a glycoprotein on host T-cells. This binding event triggers major conformational changes within the Env complex, which expose CXCR4 or CCR5 co-receptor binding sites. In turn, the gp41 fusion peptide region inserts into the host cell membrane. Subsequent refolding into a six-helix bundle brings the N and C termini of gp41 together and, in doing so, brings the virion and host cell membranes into sufficient proximity for fusion.[7–10]

The virion-cell fusion process requires poration of the viral membrane. In light of evidence to suggest that viral poration may occur in the absence of a nearby cell membrane,[11–13] we hypothesized that the intrinsic conformational change program of the metastable Env spike and proximal viral membrane in mature HIV-1 could be hijacked to cause viral membrane poration in the absence of a target cell.[11] This premise inspired earlier work in which we found that a molecule that simultaneously binds to gp120 and gp41 can impart stress to the spike, triggering viral poration.[11] With sufficient poration to drain viral contents into the extracellular milieu, the virus would be irreversibly inactivated. Indeed, we demonstrated that tethering cyanovirin, a gp120-binding lectin (MW=11.0 kDa),[14] to an exogenous segment of the gp41 MPER produces a recombinant chimeric protein that lytically inactivates HIV-1 virions.[11] Moreover, we identified Trp3, a 9-amino acid segment of the gp41 MPER truncated at the third tryptophan, as an MPER replacement.[15] Our accumulated findings with cyanovirin-Trp3 and the follow-up with microvirin-conjugated fusion proteins with Trp3 demonstrated[15,16] the overall ability to derive a new class of irreversible HIV-1 inactivators, which we have denoted as DAVEIs, ***Dual-Action Virucidal Entry Inhibitors.***

While the lectin DAVEIs are potent Env inhibitors and offer an exciting new class of irreversible virus inactivators, the complex binding modes of the lectins to multiple Env glycans and the large size of the resulting chimeras limits their development as therapeutic leads. We therefore explored the possibility to replace the lectins with small molecule gp120 inhibitors. In the study reported here, we evaluated whether the small molecule CD4 mimetic compound (CD4mc) BNM-III-170[17] could be used to engage gp120 in lieu of large lectin proteins, while allowing the corresponding small molecule-based DAVEI conjugate to retain virolytic activity as observed with lectin DAVEIs. The consequent successful derivation of the new BNM-DAVEI (vide infra) promises to simplify investigation of the mechanism of action of these small molecule DAVEIs, and at the same time to move towards a smaller, more drug-like compound.

RESULTS

Synthesis of BNM-DAVEI Variants

Access to small molecule DAVEIs first required the design of synthetic routes which permit replacement of the lectin protein of prior recombinant cyanovirin- and mirovirin-DAVEIs with BNM-III-170, a small molecule HIV-1 entry inhibitor that binds to gp120 in the Env cavity where ^{CD4}Phe43 binds[17,18] Previous investigations have demonstrated that this inhibitor mimics the functional activities of CD4, including stabilizing an open conformation of the virus Env trimer.[19]

While the open conformation induced by CD4 triggers the virus entry cascade into cells, the Env conformational cascade initiated by BNM-III-170 leads ultimately to inactivation of the virion.[17] Importantly, the gp120 binding site for BNM-III-170 has been determined at high resolution by X-ray crystallography,[17] making this binding site ideal as a component for the structurally minimized DAVEI constructs.

To this end, we have designed synthetic protocols (**Figure 1**) to incorporate the small molecule BNM-III-170 in place of the lectin incorporated in our previous generations of DAVEI constructs. A copper-catalyzed alkyne-azide click cycloaddition (CuAAC) attachment strategy[20] was employed to join the modified small molecule warhead with the Trp3 moiety developed initially for lectin DAVEIs.[15,16] The secondary amine on BNM-III-170 served as a handle for installation of a PEG-azide spacer. Crystal structures and docking studies of BNM-III-170/CD4 indicated that the secondary amine resides outside the Phe43 cavity in a relatively open area of the Env,[17] suggesting appending the large peptide moiety may not impede binding.

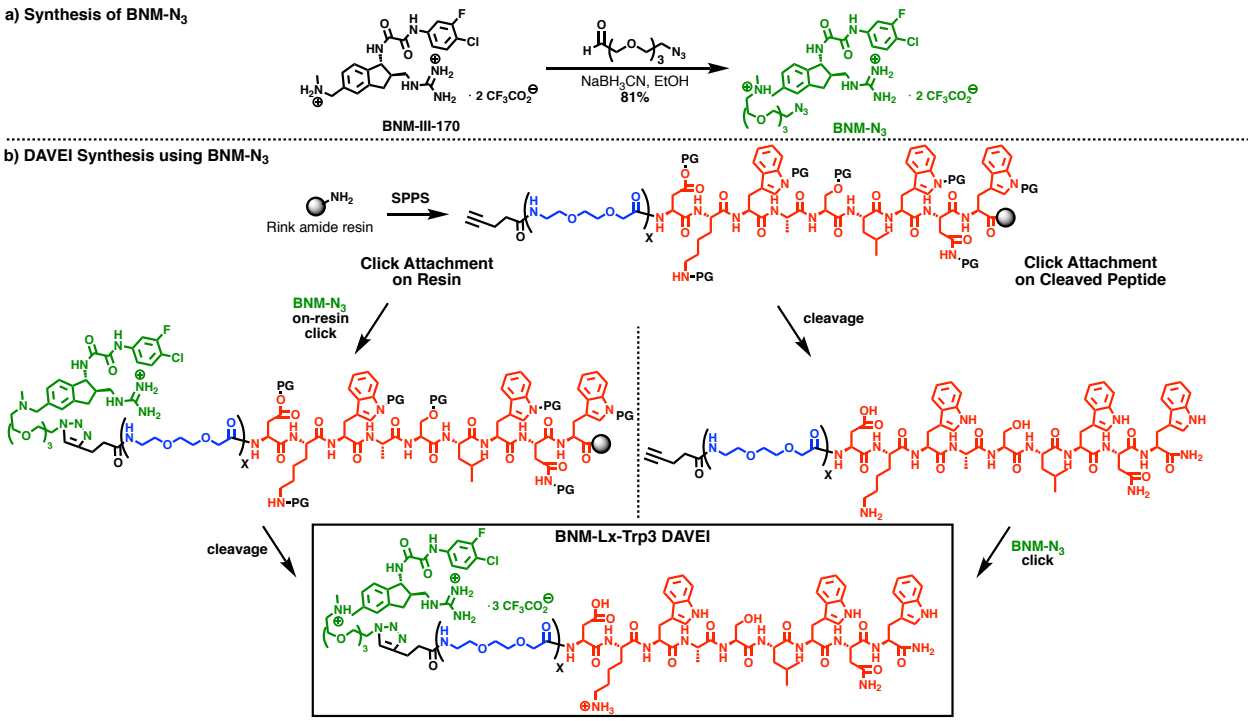

Figure 1. Alternative strategies for synthesis of small molecule DAVEIs. A. *BNM-III-170 was functionalized with an azide handle to enable CuAAC installation of the Trp3 peptide.* ***B.*** *Trp3-containing peptides incorporating different numbers of linkers and a terminal alkyne were produced using solid phase synthesis. CuAAC attachment of BNM-N₃ may be accomplished on resin followed by cleavage (left), or on the cleaved peptide (right).*

Alkyne-bearing Trp3 molecules were constructed using automated solid phase peptide synthesis. The distance between the small molecule and Trp3 components was varied via the number of ethoxyamino linker units (Lx) connecting the two components. A key feature of this attachment strategy was that a variety of linker lengths were synthesized rapidly and then, in the final step, "clicked" onto the azide-bearing small molecule warhead.

Reductive amination of BNM-III-170 with azide[21] afforded the desired small molecule azide (BNM-N_3). In turn, CuAAC attachment on the peptide alkyne-Lx-Trp3 (x = 0, 1, 3, 7) provided BNM-L0-

Trp3, BNM-L1-Trp3, BNM-L3-Trp3, and BNM-L7-Trp3, respectively. BNM-N_3 synthesis is depicted in **Figure 1a**.

Two routes of conjugate synthesis were employed. These are shown in **Figure 1b**. In both, the alkyne-Lx-Trp3 was synthesized using automated solid phase synthesis. We first generated DAVEI by performing the CuAAC on the protected, resin-bound peptide followed by deprotection on cleavage (**Figure 1b**, left). We later found that first cleaving peptide and performing the CuAAC union in solution simplified monitoring of reaction progress (**Figure 1b**, right). Purification and structural validation were carried out for all intermediates with final products employing reverse phase HPLC and mass spectrometry (see Supporting Information **Figure S1** for representative case)

Functional Properties of BNM-Trp3 DAVEIs

The BNM-DAVEI constructs were evaluated for their ability to inhibit infection and cause virolytic release of p24 from HIV-1 Bal 01 pseudoviruses. The results of these analyses are presented in **Figure 2 and Table 1**. Virolysis was determined using a p24 sandwich ELISA. All four of the covalently-linked BNM-linker-Trp3 constructs synthesized had similar infection inhibition and virolysis potencies. Importantly, the BNM-L3-Trp3 produced by the full solid phase protocol of **Figure 1** left also had strong functional potencies (inhibition of infection IC_{50} = 0.58 ± 0.09 μM, virolysis EC_{50} = 7.2 ± 0.5 μM). These results emphasize the capacity to derive lytic BNM-DAVEIs by multiple synthetic strategies. Importantly for the cell infection inhibition results, none of the compounds tested exhibited toxicity against the HOS.T4.R5 cells used in these assays (**Figure S2**).

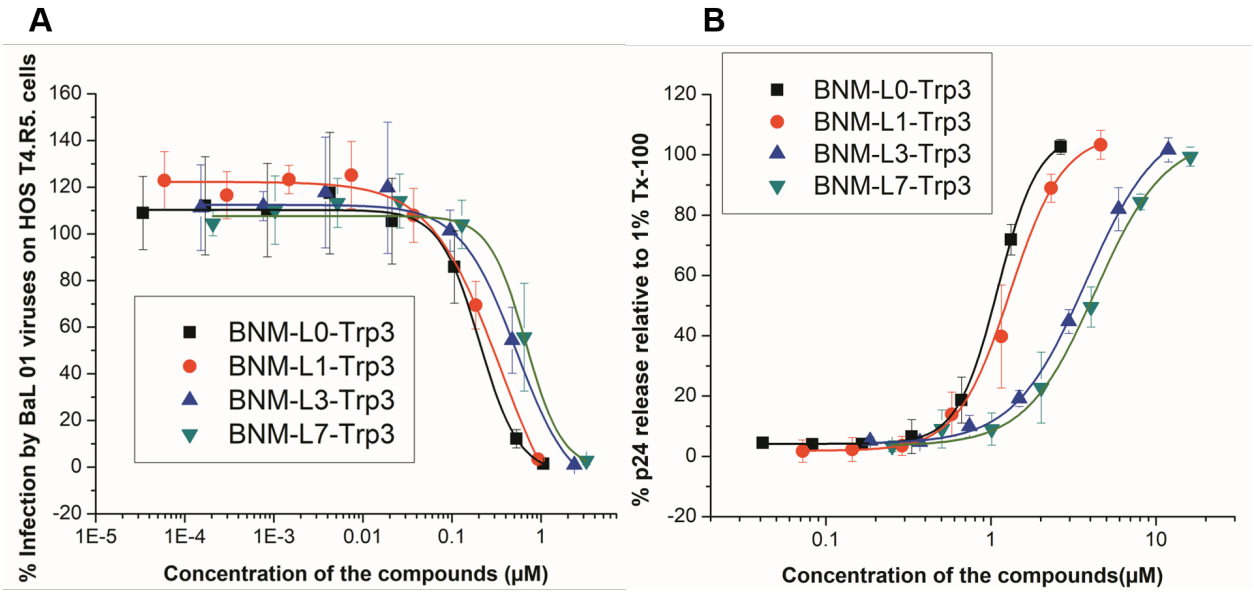

Figure 2. Infection inhibition and virolytic activities of BNM-DAVEIs. *Data shown are for the full series of linker-variant DAVEI constructs produced by combined solid phase/solution phase protocol shown in* ***Figure 1B****. Figure 2A: dose-dependence of infection inhibition, illustrating that all BNM-DAVEIs were able to inhibit infection in HOS T4.R5. cells with similar potencies. The IC_{50} values are reported in* ***Table 1****.* ***Figure 2B****: Percent of p24 released at increasing concentration of the compounds, relative to 1% Tx-100, reveals similar potencies of virolysis by the four DAVEI constructs. The EC_{50} values are reported in* ***Table 1*** *as well.*

Table 1, Functional properties of linker-variant BNM-DAVEIs.

NAME	IC_{50} (μM)	EC_{50} (μM)
BNM-III-170-N3	0.73 ± 0.04	ND
BNM-L0-Trp3	0.20 ± 0.01	1.09 ± 0.02
BNM-L1-Trp3	0.35 ± 0.20	1.30 ± 0.05
BNM-L3-Trp3	0.53 ± 0.07	3.77 ± 0.28
BNM-L7-Trp3	0.67 ± 0.19	4.29 ± 0.22
Alkyne-L3-Trp3	>> 10 No trend detected	>> 50 No trend detected

Dependence of Virolysis on Covalent Linkage of the DAVEI Domains

We evaluated the role of the covalent linkage of the small molecule CD4 mimic and peptide DAVEI components. Importantly, the azide-bearing small molecule warhead moiety BNM-N_3 and alkyne-L3-Trp3 (the unclicked linker-peptide moiety) did not cause virolysis when tested alone or as a 1:1 mixture. The simultaneous presence of a gp120-binding compound (i.e., BNM-N_3) and a gp41-binding compound is thus not sufficient to induce virolysis. It should be noted however that BNM-N_3 remains an infection inhibitor with comparable potency to the parent BNM-III-170, and that neither compound induces virolysis. The results are shown in **Figure 3.**

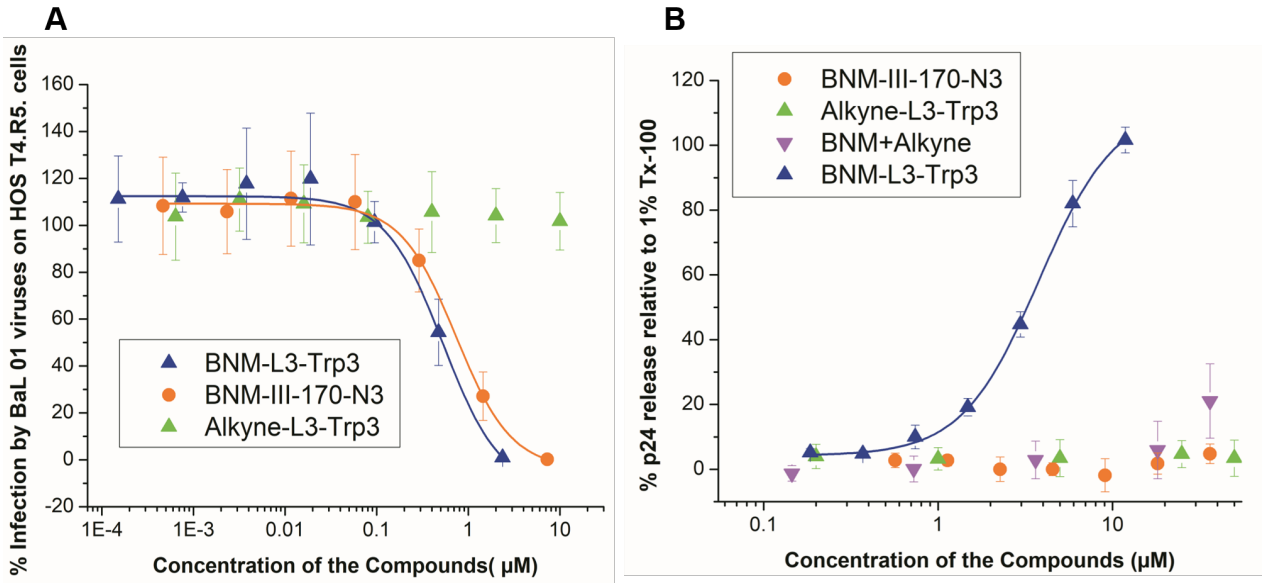

Figure 3. Dependence of BNM-DAVEI HIV-1 pseudotype virolysis on covalent linkage. ***A:*** *Inhibition of BaL.01 infection of HOS.T4.R5. cells, illustrates that BNM-L3-Trp3 retains the potency of BNM-III-170-N_3. Alkyne-L3-Trp3 as expected is not inhibitory. The IC_{50} values are as reported in* ***Table 1****.* ***B:*** *Comparison of the pseudovirus lysis activity of BNM-L3-Trp 3 versus the lack of lytic activity found with the separate components or a non-covalent mixture of the components. These data demonstrate that virolysis requires a covalent linkage between the gp120 binding group, BNM-N_3, and gp41 binding group, alkyne-L3-Trp3.*

These results emphasize the importance of our conjugation strategy, and furthermore suggest the DAVEI constructs engage the Env in a manner fundamentally different from those of the individual components prior to conjugation (see Discussion).

Molecular Simulation of BNM-DAVEI / Env Complexes

All-atom *in silico* models of BNM-DAVEI / Env complexes were generated and analyzed to complement and rationalize the results of the biological observations. A total of nine independent models of each BNM-Lx-Trp3 (x = 1, 3, 7) in a 3:1 complex with a soluble gp160 SOSIP.664 trimer (PDB ID: 5VN3)[22] were explored. Briefly, an unliganded Env model was generated from the 5VN3 entry by deleting sCD4 and 17b chains and then inserting the missing loop residues via Monte-Carlo with modeling MPER segments as α-helical continuations from residue 664. 5VN3 was selected because BNM-III-170 is known to bind to gp120 in the CD4-bound conformation.[17] Using the BNM-III-170/gp120 structure (PDB ID: 5F4P) as an alignment reference, three BNM-III-170 molecules were docked into the 5VN3 construct, and linker-Trp3 segments inserted *via* loop-relaxation Monte Carlo to steer molecular dynamics to place Trp3s next to Env MPERs. All such models were equilibrated in explicit-solvent MD simulations.

Stable complexes of both BNM-L3-Trp3 and BNM-L7-Trp3 on Env were successfully obtained. However, against a rigid Env structure, it was not possible to form a dually-engaged BNM-L1-Trp3/Env complex. A stable BNM-L1-Trp3 complex was however generated by allowing Env to move during attachment and equilibration, while artificial forces maintained the bound state of both the BNM and the Trp3. After this equilibration, the artificial forces were removed and standard MD was performed as in the BNM-L3-Trp3 and BNM-L7-Trp3 systems. In these simulations one BNM-L1-Trp3 remained completely dual-engaged, one BNM disengaged from the binding pocket, and one Trp3 drifted slightly away from MPER albeit is close to MPER and could engage again. Renderings of three representative [BNM-Lx-Trp3]/Env complexes are illustrated in **Figure 4**. These models suggest that there is sufficient flexibility in the linkers of the L3 and L7 constructs to facilitate simultaneous dual engagement with a gp41 and gp120 subunit on the CD4-activated sgp160 SOSIP.664 Env. It is important to note that the structure of the SOSIP trimer is such that the MPER nearest to a given gp120 Phe43 cavity belongs to the gp41 of the counterclockwise (looking toward viral membrane) neighboring protomer of that gp120. This modeling also illustrates that the Env trimer itself possesses sufficient flexibility to allow for the L1 DAVEI to bind stably. In the Supplemental Information, **Figure S3**, we present selected interatomic distance traces from 20ns MD trajectories of BNM-L(1,3,7)-Trp3/Env systems that indicate the stability of the bound states.

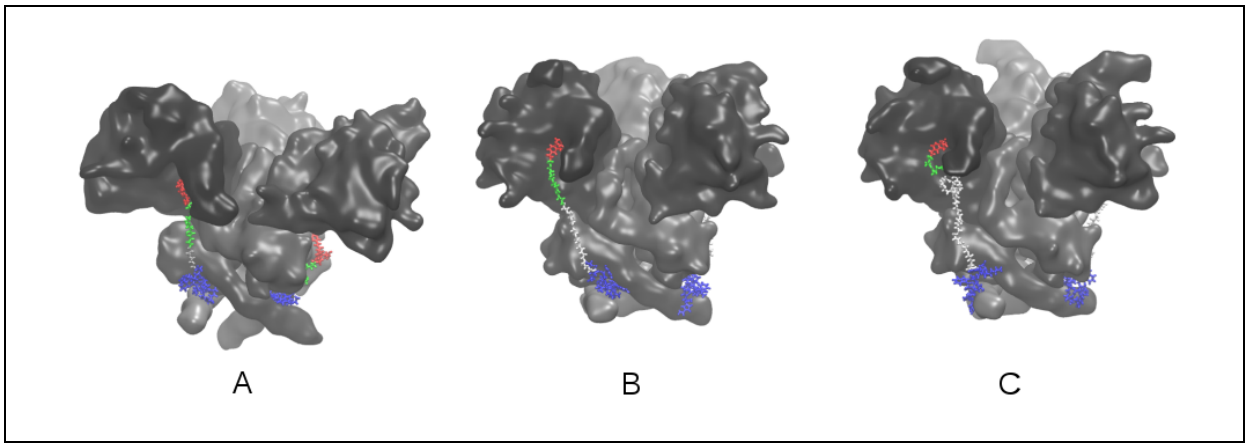

Figure 4. Models of (BNM-Ln-Trp3)$_3$/sgp160-SOSIP.664 complexes, for n = 1 (A), 3 (B), and 7 (C) linker repeat units. *Gp120 protomers are represented by darker grays, and cognate gp41's by lighter grays, BNM is shown in red, the azide spacer in green, the linker in white, and Trp3 in blue. In (A), one visible BNM has pulled out of the Phe43 binding cavity and the foreground DAVEI remains dual-engaged.*

DISCUSSION

The primary goal of the current study comprised the design, synthesis and validation of a viable synthetic strategy to small-molecule irreversible HIV-1 Env inactivators using a dual-action virolytic entry inhibitor (DAVEI) strategy. Previously, we established that DAVEIs could be produced by conjugating gp120-targeting lectin proteins to gp41-targeting small peptides. Lectin DAVEIs are potent virolytic inactivators. However, the large size and structurally ill-defined encounter of the glycan-targeting lectins to Env challenges structure-based functional optimization. We thus tested replacement of the lectin domain by the small-molecule CD4mc BNM-III-170. The latter construct has a high affinity for gp120, binds in a structurally well-defined site in the CD4 binding region, and in its own right inhibits HIV-1 cell infection at the low micromolar level. Thus, in the current work, we have established robust synthetic protocols to produce and structurally validate homogeneous BNM-DAVEI constructs (**Figure 1**). These smDAVEIs were shown not only to inhibit cell infection but also to cause HIV-1 lysis (**Figure 2**).

Importantly, the azide-bearing small molecule warhead BNM-N_3 and the alkyne-L3-Trp3 peptide did not cause significant virolysis when tested independently or when administered together as a mixture of unlinked compounds (**Figure 3**). This suggests the simultaneous presence of a gp120-binding compound and a gp41-binding compound in the absence of covalent attachment to each other is not sufficient to induce virolysis, and in turn supports the hypothesis that the stress on Env induced by the simultaneous binding of the two conjugate components is required for lysis. It should also be noted that BNM-III-170 and BNM-N_3 retain potent inhibition of viral infection in the presence of the Trp3 peptide.

From the finding that both the small molecule and peptide components must be covalently linked in order for BNM-DAVEIs to cause virolysis, we may infer that simultaneous binding of gp120 and gp41 likely is required. That is, deformation and stress to the Env protein complex resulting from simultaneous engagement may be an essential requirement for lysis to occur. In turn, one could surmise that there exists a balance between optimal linker length (i.e., structure) to cause stress of the Env complex, while also enabling simultaneous engagement of the two DAVEI components at their respective gp120 and gp41 binding sites. We examined BNM-DAVEI constructs with

differing linker lengths from L0 to L7. Lytic activity was significant in all cases, with fractionally greater potency seen with the shortest (L1) or no (L0) linker length. This finding made it important to assess how the BNM-DAVEI variants could bind to the Env structure. All-atom computational modeling (**Figures 4 and S3**) revealed that only L3 and L7 BNM-DAVEIs were able to engage the Env conformation represented in the CD4/17b-bound cryo-EM structure of sgp160 SOSIP.664,[22] while under simulation that Env structure also displayed sufficient flexibility to permit stable binding of the L1 variant. Though instructive, these models are still somewhat speculative because unlike BNM-III-170, there is as yet no precise structural evidence of the Trp3 binding site. Our prior work with Trp3 strongly suggests specific binding to Env MPER, yet the lack of MPER on the sgp160 SOSIP.664 construct had to be modeled.[11,15] We maintain that the general picture of how DAVEIs bind as presented here is supported by existing data, but recognize that newer Env structures (in particular, those containing residues C-terminal to 664, including MPER) may necessitate updates to these models.

OVERALL IMPACT

The work described here establishes a transition from recombinant protein engineering to synthetic chemistry in the development of small molecule dual-action virolytic entry inhibitors (DAVEIs) of HIV-1. While our recombinant approach incorporating lectin protein warheads demonstrated proof-of-concept that Env metastability could be harnessed to irreversibly inactivate HIV-1 Env and kill virus particles, it leaves open questions around the mechanism of action of DAVEIs. Moreover, the utility of large protein therapeutics is limited. The development of the small-molecule BNM-DAVEIs presented here is thus expected to drive forward efforts in both of these directions. Since the BNM-III-170 binding site in gp120 has been defined at high resolution, deriving structural models such as those in **Figure 4** to drive future design and synthetic optimization will now be feasible. In addition, the feasibility to develop further the Trp3 domain, for example by stabilization via stapling or replacement by *de novo* surrogate small molecules, opens the way to more drug-like DAVEIs. Finally, because the target of DAVEIs is the membrane-embedded HIV-1 Env, there is the strong potential for using DAVEIs to kill HIV-1-infected cells displaying Env on their plasma membranes. These advances thus hold promise for use of DAVEIs for irreversible inactivation of the Env complex on both HIV-1 virus and virus-producing cells as strategies for HIV-1 eradication.

METHODS

Synthesis

BNM-III-170-N_3. To BNM-III-170 (35 mg, 0.052 mmol) under N_2 at room temperature was added the aldehyde[21] (17 mg, 0.078 mmol, 1.5 eq) as a 0.1 M solution in 5:3 MeOH/EtOH, followed by $NaBH_3CN$ (0.040 g, 0.062 mmol, 1.2 eq). The reaction mixture was stirred overnight. The crude mixture was concentrated, dissolved in 1.5 mL acetonitrile, 1.5 mL water and 0.2 mL TFA. HPLC purification (15 mL/min, 30-80% acetonitrile/water + 0.1% TFA, 7 min gradient) afforded BNM-N_3 (36 mg, 81% yield). ^{1}H NMR (500 MHz, acetone-d6) δ 11.74 (bs, 1H), 10.31 (s, 1H), 8.83 (m, 2H), 8.01 (dd, J = 2.4, 11.5 Hz, 1H), 7.95-7.60 (bs, 3H), 7.74 (m, 1H), 7.53 (m, 2H), 7.48 (d, J = 7.7 Hz, 1H), 7.32 (d, J = 7.7 Hz, 1H), 5.33 (t, J = 8.7 Hz, 1H), 4.50 (d, J = 48.5 Hz, 2H), 3.99 (t, J = 4.9 Hz, 2H), 3.74-3.52 (m, 13H), 3.52-3.38 (m, 2H), 3.37 (t, J = 4.9 Hz, 2H), 3.31 (dd, J = 8.1, 16.0 Hz, 1H), 2.99 (dd, J = 8.1, 15.7 Hz, 1H), 2.93 (s, 3H), 2.86 (dd, J = 9.0, 16.0 Hz, 1H). ^{13}C NMR (500 MHz, acetone-d6) δ 34.28, 39.93, 43.86, 46.92, 50.57, 54.59, 57.96, 59.86, 64.84, 69.84, 70.20, 70.27, 70.35, 70.38, 108.39, 108.60, 115.45, 115.59, 117.11, 124.55, 127,90, 130.03, 130.23, 130.80, 138.19, 138.27, 142.81, 143.91, 156.78, 158.24, 158.41, 158.51, 158.72, 159.92, 160.26. AMM ESI 648.2819 observed (648.2825 theoretical).

IR (neat) νmax = 3357.9, 2918.7, 2874.4, 2359.5, 2340.2, 2104.4, 1675.8, 1513.4, 1428.0, 1202.9, 1129.6, 668.2, 456.1, 438.7, 421.9, 406.9. $[\alpha]_D^{23}$ = 20 ° (*c* 0.10, CH_3CN).

BNM-L0-Trp3*.* Water and *t*-butanol were sparged with nitrogen for four hours. To BNM-III-170-N_3 under nitrogen in a round bottom flask was added a 9 M solution of alkyne-L0-Trp3 in 1:1 *t*-butanol:water (2 mL), then a solution of sodium ascorbate (0.036 g, 0.180 mmol, 10 eq), $CuSO_4$ $5H_2O$ (0.018 g, 0.072 mmol, 4 eq), and THPTA (0.016 g, 0.036 mmol, 2 eq) in 1:1 *t*-butanol:water (1 mL). The reaction mixture was heated to 50°C overnight. Reaction progress was monitored by LC/MS. The crude reaction mixture was transferred with 1:1 acetonitrile/water, filtered through sand, and concentrated to 3 mL. The crude diluted mixture was purified by reverse phase HPLC (18 mL/min, 25-60% acetonitrile/water, 11 min) to afford 3.93 mg of BNM-L0-Trp3 (10%). AMM ESI M+2H/2 966.4527 obs. (966.4495 theoretical).

Alkyne-L1-Trp3 [Z-X-D-K-W-A-S-L-W-N-W]*.* The above peptide (Z = 4-pentynoic acid, X = 8-amino-3,6-dioxaoctanoic acid) was synthesized using a Liberty Blue solid phase peptide synthesizer. The resin-bound peptide was transferred to a synthesis vessel and washed three times with dichloromethane. A pre-mixed solution of TFA (8 mL), TIPS (1 mL), and water (1 mL) was added. The resin-bound peptide was agitated for 90 minutes, drained, and concentrated with a nitrogen stream. The crude peptide was dissolved in acetonitrile/water and purified by HPLC (15 mL/min, 35-65% H_2O/ACN + 0.1% TFA, 13 min gradient).

BNM-L1-Trp3*.* DMF and water were sparged with nitrogen for five hours. A buffer solution (1.45 g guanidine hydrochloride and 0.07 g sodium hydrogen phosphate in 2.5 mL water) was prepared. To the alkyne (0.020 g, 0.010 mmol, 1 eq) in a microwave reactor vessel under nitrogen was added a solution of BNM-III-170-N_3 (0.009 g, 0.010 mmol, 1 eq) in DMF (1 mL) and buffer (1 mL). To this solution were added sodium ascorbate (0.12 g, 0.60 mmol, 60 eq) and $CuSO_4$ $5H_2O$ (0.050 g, 0.20 mmol, 20 eq). The reaction vessel was sealed and subjected to microwave irradiation at 60°C for 13 h. The crude reaction mixture was filtered through sand and diluted with 1:1 acetonitrile/water to 5 mL. The crude diluted mixture was purified by reverse phase HPLC (18 mL/min, 30-60% acetonitrile/water, 9 min) to afford 2.51 mg of BNM-L1-Trp3 (10%). MALDI-TOF: 2075.214

BNM-L3-Trp3 (on resin CuAAC)*.* The resin-bound alkyne-L3-Trp3 peptide was placed in a reaction vessel. DMF was drained and the resin was washed with ACN. ACN was then drained. 1 equivalent of the azido-intermediate was dissolved in least amount of ACN. The azide solution was added to the click reaction solvent mixture: 6 mL ACN, 4 mL H_2O, 1 mL DIEPA, 0.5 mL pyridine. 1 equivalent CuI was added to the resin-peptide and then add the solvent mixture was added to the reaction vessel. The mixture was shaken at r.t. for 12 h. and then was washed with 5% HCl (3 x 50 mL), DMF (3 x 50 mL) and DCM (3 x 50 mL). Cleavage/ deprotection of the BNM-L3-Trp3 from resin was the performed. A pre-cooled mixture of (8 mL TFA+1 mL H_2O+1mL TIPS) was added to the resin in a 25 mL flask and stirred at r.t. for 2 h. The mixture was then filtered; the filtrate was concentrated by a gentle N_2 stream. A pre-cooled ether was added to the concentrated filtrate to precipitate the peptide and the mixture was vortexed and centrifuged. Ether was drained and the solid peptide was dried before re-dissolving in (ACN/H_2O/0.1% TFA) for HPLC purification (prep C18 RP column using gradient 5% ACN to 95% in 45 min, 10 mL/min flow rate, 210 nm). Yield: 78%. HPLC homogeneity: 96.7%. Calculated m/z; 1185.02, 790.35, 593.01. Observed m/z; 1185.27, 790.48, 593.26.

Alkyne-L3-Trp3 [Z-X-X-X-D-K-W-A-S-L-W-N-W]*.* The above peptide (Z = 4-pentynoic acid, X = 8-amino-3,6-dioxaoctanoic acid was synthesized using a Liberty Blue solid phase peptide synthesizer. The resin-bound peptide was transferred to a synthesis vessel and washed three times with dichloromethane. A pre-mixed solution of TFA (8 mL), TIPS (1 mL), and water (1 mL)

was added. The resin-bound peptide was agitated for 90 minutes, drained, and concentrated with a nitrogen stream. The crude peptide was dissolved in acetonitrile/water and purified by HPLC (15 mL/min, 30-70% H_2O/ACN + 0.1% TFA, 13 min gradient)

BNM-L3-Trp3 (solution phase CuAAC). A 1:1 solution of DMF/H_2O was sparged with nitrogen for two hours. To alkyne-L3-Trp3 (0.020 g, 0.011 mmol, 1 eq) in a round bottom flask under nitrogen was added 0.1 mL of a 0.1 M solution of BNM-III-170 (0.010 g, 0.011 mmol, 1 eq) in sparged 1:1 DMF/H_2O. To this solution was added a pre-mixed catalyst solution comprised of THPTA (0.019 mg, 0.11 mmol, 10 eq), $CuSO_4$ $5H_2O$ (0.011 g, 0.044 mmol, 4 eq) and sodium ascorbate (0.022 g, 0.044 mmol, 4 eq) in 1 mL 1:1 sparged DMF/H_2O. The crude reaction mixture was transferred with 1:1 water/acetonitrile and filtered through sand. The crude mixture was purified by reverse phase HPLC (15 mL/min, 30-70% H_2O/ACN + 0.1% TFA, 15 min) to afford 4.08 mg of BNM-L3-Trp3 (13%). AMM ESI M+2H/2 1184.0615 obs. (1184.0604 theoretical).

Alkyne-L7-Trp3 [Z-X-X-X-X-X-X-D-K-W-A-S-L-W-N-W]. The above peptide (Z = 4-pentynoic acid, X = 8-amino-3,6-dioxaoctanoic acid was was synthesized using a Liberty Blue solid phase peptide synthesizer. The resin-bound peptide was transferred to a synthesis vessel and washed three times with dichloromethane. A pre-mixed solution of TFA (8 mL), TIPS (1 mL), and water (1 mL) was added. The resin-bound peptide was agitated for 90 minutes, drained, and concentrated with a nitrogen stream. The crude peptide was triturated with 3 x Et_2O, dissolved in acetonitrile/water and purified by HPLC (15 mL/min, 33-55% H_2O/ACN + 0.1% TFA, 15 min gradient).

BNM-L7-Trp3. DMF and water were sparged with nitrogen for five hours. A buffer solution (0.58 g guanidine hydrochloride and 0.028 g sodium hydrogen phosphate in 1 mL water) was prepared. To the alkyne (0.027 g, 0.012 mmol, 1 eq) and BNM-III-170-N_3 (0.013 g, 0.015 mmol, 1.3 eq) in a microwave reactor vessel under nitrogen was added buffer solution (2 mL), then sodium ascorbate (0.14 g, 0.70 mmol, 60 eq) and $CuSO_4$ $5H_2O$ (0.058 g, 0.23 mmol, 20 eq). The reaction vessel was sealed and subjected to microwave irradiation at 60°C for 3 h, then stirred at RT for 24 hours. The crude reaction mixture was filtered through sand and diluted with 1:1 acetonitrile/water to 3.5 mL. The crude diluted mixture was purified by reverse phase HPLC (18 mL/min, 30-60% acetonitrile/water, 9 min) to afford 8.52 mg of BNM-L7-Trp3 (22%). MALDI-TOF: 2946.027

Functional analyses

Pseudovirus production
Recombinant HIV-1 pseudoviruses were produced using HEK-293T cells. Approximately 3 million cells/flask were seeded. 24 hours later, the cells were transfected with 8 µg of either HIV-1 BaL-01 envelope plasmid and 4 µg of NL4-3 backbone sequence corresponding to an envelope-deficient pNL4-3 luc^+, env^- developed by N. Landau. At 48 hours post transfection, the supernatants were collected, filtered through 0.2 µm filter, and purified through a 6-20% iodixanol gradient.

HOS.T4.R5 Cells
Modified human osteoscarcoma cells expressing both the receptor CD4 and coreceptor CCR5 (HOS.T4.R5) were obtained from Dr. Nathaniel Landau through the NIH AIDS Reagent Program.

Cell Infection Inhibition Assay
Pseudoviral infection assays were used to validate the infectivity of the pseudo viruses produced as well as to determine the infection inhibition potency of the inhibitors synthesized. HOS.T4.R5

cells were seeded in a 96 well tissue culture plate at 7500 cells, 100 µl/well and cultured at 37 ºC with 5% CO_2. 24 hours after seeding, samples containing serial dilutions of inhibitors with purified pseudo virus in a 1:1 ratio were incubated for 30 mins at 37ºC and added to the plates. After 24 hours of infecting, a growth media wash step was performed. 24 hours after media change, the plates were washed with 1x DPBS solution and the cells were lysed with 1X lysis buffer. The lysate was then transferred to a white plate and mixed with lysis buffer and luciferin salt, before measuring the luminescence using a Luminescence reader. The signals were plotted as a function of virus control, where the cells were treated with just the same dilution of virus. The analysis will be performed using Origin v.8.1 (OriginLab, Northampton, USA) to calculate the IC_{50} values.

Analysis of Cell Infection Inhibition Data

The data from the dose – dependent measurements to determine IC_{50} values were generated by a sigmoidal curve fitting using the Origin software, as previously described.[23–25]

Virolysis Assay
In order to analyze the ability of the inhibitors to cause virolysis upon its interaction with pseudotype HIV-1 Bal 01. viruses, a sandwich ELISA assay was used where the amount of p24 released by the viruses was quantified. High binding polystyrene ELISA plates were coated with 50ng/well of mouse anti-p24 for 2 hours at room temperature followed by blocking with 3% BSA overnight at 4ºC. Serial dilution of inhibitors being tested were mixed with pseudoviruses in 1:1 ratio, incubated at 37ºC for 12 hours before a 2-hour spin at 15000xg at 4ºC on a tabletop centrifuge. Following the spin, the supernatant was collected and loaded on the ELISA plate to be tested for p24 content. The samples were incubated on the plate at 4ºC overnight. Following this, the plate was washed with PBS-T three times for 5 mins each before being quantified using a primary antibody, anti-rabbit p24, and secondary antibody, anti-rabbit IgG fused to horseradish peroxidase (HRP) using a 1:3000 dilution. The activity of HRP conjugate binding was determined by the addition of o-phenylenediamine dihydrochloride (OPD), before reading the signal at 450nm using a transmission plate reader. The signals were plotted as a function of p24 released where a lysed virus control treated with 1% triton x-100 will be used as the 100% value. The analysis was performed using Origin v.8.1 (OriginLab, Northampton, USA) to calculate the IC_{50} values.

Virolysis Data Analysis
The p24 content released from pseudoviruses after their interaction with inhibitors was used to determine virolysis. Here the controls are intact virus and lysed virus. The intact virus are samples where the viruses are treated with only buffer. While, in lysed virus sample the viruses are treated with 1% Triton X -100 and used as the 100% control. The dose dependent data were analyzed using Origin to generate EC_{50} values.

Molecular Simulations

Generation and testing of atomically precise models of Env/(BNM-Lx-Trp3)$_3$ complexes.
Molecular model-building in this work is based on the assumptions that (1) the BNM moiety of a DAVEI binds to Env trimer as does a standalone BNM in core monomeric gp210,[17] and (2) the Trp3 moiety interacts with residues near the 2F5 epitope on MPER.[15] No current trimeric model of Env displays both of these binding sites, so the cryo-EM structure of the CD4- and 17b-bound SOSIP trimer (PDB ID 5VN3)[22] was selected as a base model onto which MPER residues 665 to 682 (HXB2 numbering) of each gp41 protomer are added on as a helical extension of the corresponding C-terminal heptad repeat. To generate an initial complex of Env/(BNM-Lx-Trp3)$_3$, (1) a BNM molecule is aligned into its crystallographic binding site on each protomer; (2) the

spacer and linker moieties are grown from each BNM using randomly chosen dihedral angles, and (3) a series of vacuum-phase Monte Carlo and steered molecular dynamics simulations are used to guide each molecule's Trp3 moiety to contact the nearest gp41 MPER while avoiding steric clashes. Further details on this series of guiding simulations is given in the Supporting Materials. For each linker degree n, three replica systems, each with three independent BNM-Ln-Trp3 dockings, were generated, so that the dataset for each n comprises nine independent docking trials.

Molecular dynamics trajectories. Each replica system was solvated with explicit water and neutralized with counterions in a box of size 150 x 150 x 135 $Å^3$ (roughly 310,000 total atoms). After a short series of equilibration runs (detailed in the Supporting Information), production MD was performed for 20 ns on each system. These simulations were run using NAMD 2.12[26] and the CHARMM36 force field[27] (with BNM parameterized using paramchem in the CHARMM General Force Field)[28], with the Langevin thermostat and barostat and a cutoff of 10 Å.

Acknowledgement

We thank Harry C. Bach and Marg V. Rajpara for their laboratory assistance with peptide synthesis and infection inhibition assays.

Funding

This project was supported by the NIH grants R01: GM115249, P01: P01 GM 56550 and P01 AI150471.

Citations

1. UNAIDS. AIDS by the numbers. *AIDS by the Numbers 2015* 1–25 (2016). doi:JC2571/1/E
2. Kaiser Family Foundation. U.S. Federal Funding for HIV/AIDS: Trends Over Time. at <http://files.kff.org/attachment/Fact-Sheet-US-Federal-Funding-for-HIVAIDS-Trends-Over-Time>
3. Posse, M., Meheus, *et al.* Barriers to access to antiretroviral treatment in developing countries: A review. *Trop. Med. Int. Heal.* **13,** 904–913 (2008).
4. Swidorski, J. J. *et al.* Inhibitors of HIV-1 attachment: The discovery and structure-activity relationships of tetrahydroisoquinolines as replacements for the piperazine benzamide in the 3-glyoxylyl 6-azaindole pharmacophore. *Bioorganic Med. Chem. Lett.* **26,** 160–167 (2016).
5. WHO. WHO HIV Drug Resistance Report. (2012). at <http://www.who.int/hiv/pub/drugresistance/report2012/en/>
6. Herschhorn, A. *et al.* A broad HIV-1 inhibitor blocks envelope glycoprotein transitions critical for entry. *Nat. Chem. Biol.* **10,** 845–52 (2014).
7. Chan, D. C., *et al.*HIV entry and its inhibition. *Cell* **93,** 681–684 (1998).
8. Doms, R. W., *et al.* Unwelcomed guests with master keyes: How HIV uses chemokine receptors for cellular entry. *Virology* **235,** 179–190 (1997).
9. Pierson, T. C., *et al. Cellular Factors Involved in Early Steps of Retroviral Replication* 1–27 (2003). doi:10.1007/978-3-642-19012-4_1
10. Wilen, C. B., *et al.* HIV: Cell binding and entry. *Cold Spring Harb. Perspect. Med.* **2,**

(2012).

11. Contarino, M. *et al.* Chimeric cyanovirin-MPER recombinantly engineered proteins cause cell-free virolysis of HIV-1. *Antimicrob. Agents Chemother.* **57,** 4743–4750 (2013).

12. Bennett, A. *et al.* Cryoelectron tomographic analysis of an HIV-neutralizing protein and its complex with native viral gp120. *J. Biol. Chem.* **282,** 27754–27759 (2007).

13. Dimitrov, A. S., *et al.* Early Intermediates in HIV-1 Envelope Glycoprotein-mediated Fusion Triggered by CD4 and Co-receptor Complexes. *J. Biol. Chem.* **276,** 30335–30341 (2001).

14. Gustafson, K. R. *et al.* Isolation , Primary Sequence Determination , and Disulfide Bond Structure of Cyanovirin-N , an Anti-HIV (Human Immunodeficiency Virus) Protein from the Cyanobacterium Nostoc ellipsosporum. *Biochem. Biophys. Res. Commun.* **238,** 223–228 (1997).

15. Parajuli, B. *et al.* Lytic Inactivation of Human Immunodeficiency Virus by Dual Engagement of gp120 and gp41 Domains in the Virus Env Protein Trimer. *Biochemistry* **55,** 6100–6114 (2016).

16. Parajuli, B. *et al.* Restricted HIV-1 Env glycan engagement by lectin-reengineered DAVEI protein chimera is sufficient for lytic inactivation of the virus. (2018).

17. Melillo, B. *et al.* Small-Molecule CD4-Mimics: Structure-Based Optimization of HIV-1 Entry Inhibition. *ACS Med. Chem. Lett.* **7,** 330–334 (2016).

18. Courter, J. R. *et al.* Structure-Based Design, Synthesis and Validation of CD4-Mimetic Small Molecule Inhibitors of HIV - 1 Entry: Conversion of a Viral Entry Agonist to an Antagonist. *Acc. Chem. Res.* **47,** 1228–1237 (2014).

19. Munro, J. B. *et al.* Conformational dynamics of single HIV-1 envelope trimers on the surface of native virions. *Science* **346,** 759–63 (2014).

20. Rostovtsev, V. V., *et al.* A Stepwise Huisgen Cycloaddition Process: Copper(I)-Catalyzed Regioselective 'Ligation' of Azides and Terminal Alkynes. *Angew. Chemie Int. Ed.* **41,** 2596–2599 (2002).

21. Park, K. D., *et al.* Useful Tools for Biomolecule Isolation, Detection, and Identification: Acylhydrazone-Based Cleavable Linkers. *Chem. Biol.* **16,** 763–772 (2009).

22. Ozorowski, G. *et al.* Open and closed structures reveal allostery and pliability in the HIV-1 envelope spike. *Nature* **547,** 360–361 (2017).

23. Bailey, L. D. *et al.* Disulfide Sensitivity in the Env Protein Underlies Lytic Inactivation of HIV-1 by Peptide Triazole Thiols. *ACS Chem. Biol.* **10,** 2861–2873 (2015).

24. Bastian, A. R. *et al.* Interactions of peptide triazole thiols with Env gp120 induce irreversible breakdown and inactivation of HIV-1 virions. *Retrovirology* **10,** (2013).

25. Bastian, A. R. *et al.* Mechanism of multivalent nanoparticle encounter with HIV-1 for potency enhancement of peptide triazole virus inactivation. *J. Biol. Chem.* **290,** 529–543 (2015).

26. J.C., P. *et al.* Scalable molecular dynamics with NAMD. *J. Comput. Chem.* **26,** 1781–1802 (2005).

27. Best, R. B. *et al.* Optimization of the additive CHARMM all-atom protein force field targeting improved sampling of the backbone φ, ψ and side-chain χ1 and χ2 Dihedral Angles. *J. Chem. Theory Comput.* **8,** 3257–3273 (2012).

28. Vanommeslaeghe, K. *et al.* CHARMM general force field: A force field for drug-like molecules compatible with the CHARMM all-atom additive biological force fields. *J. Comput. Chem.* **31,** 671–690 (2010).